Understanding Water Adsorption in Cu-BTC Metal-Organic Frameworks

ARTICLE *in* THE JOURNAL OF PHYSICAL CHEMISTRY C · OCTOBER 2008

Impact Factor: 4.77 · DOI: 10.1021/jp806363w

3 AUTHORS, INCLUDING:

J. M. Castillo
Universidad Pablo de Olavide
21 PUBLICATIONS **435** CITATIONS
SEE PROFILE

Sofia Calero
Universidad Pablo de Olavide
164 PUBLICATIONS **3,074** CITATIONS
SEE PROFILE

THE JOURNAL OF PHYSICAL CHEMISTRY C LETTERS

2008, *112,* 15934–15939
Published on Web 09/19/2008

Understanding Water Adsorption in Cu−BTC Metal−Organic Frameworks

Juan Manuel Castillo,[†,‡] Thijs J. H. Vlugt,[‡] and Sofía Calero*[,†]

Department of Physical, Chemical, and Natural Systems, University Pablo de Olavide, Ctra. Utrera km. 1. 41013 Seville, Spain, and Process & Energy Laboratory, Delft University of Technology, Leeghwaterstraat 44, 2628CA Delft, The Netherlands

Received: July 18, 2008; Revised Manuscript Received: September 2, 2008

Molecular simulations were performed to study the adsorption behavior of water in the metal−organic framework Cu−BTC. This is one of the better-known materials of this type that is stable upon water adsorption/desorption. The charge of the framework atoms was fitted to reproduce the available experimental adsorption isotherm. This new set of interaction parameters was used to calculate Henry coefficients as well as the energies, entropies, and enthalpies for the different adsorption sites. Our simulations show that water has a surprisingly large affinity for the metal center in Cu−BTC compared to other that for molecules like carbon dioxide, nitrogen, oxygen, or hydrocarbons. This particular behavior could be further exploited for the separation of water from other compounds.

Introduction

Metal−organic frameworks (MOFs) are a new type of materials that are attracting a great deal of attention as potential catalysts or materials for gas storage or separation.[1−8] They exhibit a periodic structure with pores, channels, big void spaces, and a large surface area. Due to the wide range of potential linker molecules, the geometry of the framework can, in principle, be specifically designed for one particular application.[9−12] However, severe problems might arise after synthesizing a new MOF. For example, the framework may be unstable upon solvent removal after synthesis, reducing the applicability as an adsorbent, or it may change its structure by widening or narrowing the pores significantly.[13,14] The solvent molecules used in the synthesis process have a crucial effect on the formation of the final structure,[15] and water is easily encapsulated in some MOFs through coordination bonds or hydrogen bonds.[16,17] In all of these processes, the interaction of water−MOF is a key property. Understanding the interactions between water and different MOFs will be a major step forward in the design of new tailor-made materials for specific applications.

MOFs with the same type of central metal atom may have similar properties. For example, Zn-containing structures are, in general, very sensitive to water. Although a few of them are stable,[18] most of them decompose after the adsorption of water or even in the presence of moist air.[19,20] This instability is a serious limitation to the potential industrial application of Zn-containing MOFs, for example, for hydrogen storage.[20,21] In contrast, Cu-containing MOFs are often water stable[22−25] and therefore more interesting from an industrial point of view.

We are using molecular simulations to explain the water adsorption behavior in Cu−BTC (BTC: benzene-1,3,5-tricarboxylate). This MOF has attracted a great deal of attention since it was first reported by Chui et al.[22] in 1999. The framework consists of a metal coordination polymer based on Cu as the center and BTC as the linker molecule, resulting in eight octahedral side pockets per unit cell at the vertices, built from the BTC molecules linked by dimeric cupric tetracarboxylate units; see Figure 1. To date, studies of the interactions of water with MOFs are extremely scarce, and only a few studies related to water in Cu−BTC have been published, most of them being experimental works. These studies deal with water adsorption,[20,26] water saturation,[27] and the structural changes provoked by the adsorption and distribution of water in the structure.[28] Cu−BTC is also of potential interest for separating polar from nonpolar components.[7] Simulations studies on Cu−BTC are scarce too, and most of them are focused on adsorption and separation of hydrocarbons and some small molecules such as Ar, N_2, O_2, and CO_2.[7,29−32] There is only one simulation study of water in

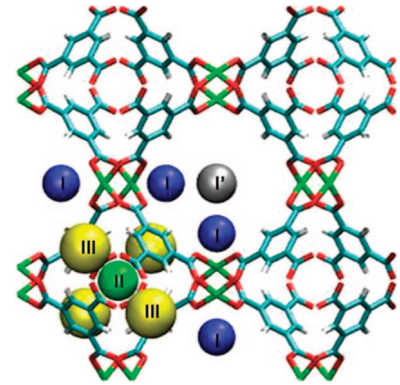

Figure 1. Structure of Cu−BTC showing the BTC molecules forming octahedra at the vertices linked by $Cu_2(COO)_4$ units; blue, carbon; white, hydrogen; green, copper; red, oxygen. The adsorption sites are also shown; site I, region close to the Cu atoms of the framework (blue spheres); site II, center of the octahedral side pockets (green sphere); site III, windows of the octahedral side pockets (yellow spheres); site I′, center of the big Cu−BTC cages (gray sphere). The size and shape of the sites do not correspond to the size and shape of the spheres.

* To whom correspondence should be addressed. E-mail: scalero@upo.es.
† University Pablo de Olavide.
‡ Delft University of Technology.

10.1021/jp806363w CCC: $40.75

MOFs that deals with the interactions of SPC water with MOF-5.[19] This work is, to the best of our knowledge, the first simulation study of water reproducing experimental adsorption isotherms in MOFs.

Simulation Details

The adsorption isotherms of water in Cu−BTC were computed using grand-canonical Monte Carlo (GCMC) simulations. The gas phase can be considered as an ideal gas as we only considered pressures of at most 275 Pa. The insertion and deletion of water molecules in the system were performed using the configurational-bias Monte Carlo technique.[33] The Henry coefficients, energies, enthalpies, and entropies of adsorption were computed from MC simulations in the NVT ensemble. During these simulations, the test particle method was used to collect information on the Rosenbluth weight. Detailed information about this method can be found elsewhere.[34−36] The MC moves were performed in cycles, and in each cycle, one of the following trial moves was selected at random for each water molecule: translation, rotation, regrow at a random position, or insertion or deletion of a water molecule (only for simulations in the grand-canonical ensemble). We used at least 10^9 Monte Carlo moves to collect data. Coulombic interactions were computed using the Ewald summation with a relative precision of 10^{-6}.

The water model used in this study is the Tip5pEw, which was parametrized for use with the Ewald summation.[37] The experimental liquid density of water at 298 K (997.0 kg/m^3)[38] is well reproduced by simulations using this interaction potential (998.0 kg/m^3), as well as the maximum of density at around 4 °C. The heat of vaporization of this model equals 43.4 kJ/mol, while the experimental value is 43.9 kJ/mol.[37]

To construct the crystallographic atomic positions of the framework, we used the crystal structure of Chui et al.[22] This structure includes axial oxygen atoms weakly bonded to the Cu atoms, corresponding to water ligands. This adsorption study was performed on a dehydrated Cu−BTC; therefore, it was adopted with these oxygen atoms removed from the crystal structure. Cu−BTC was modeled as a rigid structure with Lennard-Jones parameters taken from the DREIDING force field,[39] except those for Cu that were taken from the UFF force field.[40] The framework was kept rigid during the calculations, as it has been shown that this structure is quite rigid and that water adsorption is reversible.[41] Note that the development of flexible models for MOFs is still extremely complex, as shown by Dubbeldam et al. for the IRMOF family.[42] A single unit cell ($a = b = c = 26.343$ Å) was used in the simulations. The unit cell contained 624 atoms, of which 48 were copper, 192 oxygen, 96 hydrogen, and 288 carbon (the latter classified in three groups depending on the neighboring atoms; Ca, next to two oxygen atoms; Cb, between three carbons; and Cc, linked to one hydrogen). The crystallographically different atoms are depicted in Figure 2. The Lennard-Jones interactions between the different atoms of the system were calculated using the Lorentz−Berthelot mixing rules. Lennard-Jones interactions are truncated and shifted at 12 Å. This work highlights the importance of the Coulombic interactions for the determination of adsorption properties of water in MOFs. We demonstrate that experimental isotherms in this MOF can be reproduced exactly with molecular simulations using available force fields as a starting point. The partial charges of the framework atoms are slightly altered to fit the experimental data.

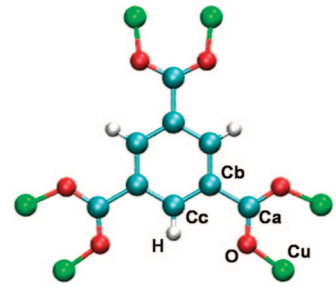

Figure 2. The crystallographically different atoms in Cu−BTC as defined in this work. We consider the following types of carbon atoms: Ca, linked to two oxygen atoms; Cb, linked to other three carbon atoms; Cc, linked to one hydrogen atom.

TABLE 1: Sets of Point Charges of Cu−BTC Used in This Work (in units of e)[a]

	Cu	O	Ca	Cb	*Cc*	H
set I	1.0	−0.6	0.7	0.0	−0.15	0.15
set II	1.2	−0.6	0.475	0.125	−0.15	0.15
set III	1.224	−0.612	0.4845	0.1275	−0.153	0.153
set IV	1.248	−0.624	0.494	0.13	−0.156	0.156
set V	1.272	−0.636	0.5035	0.1325	−0.159	0.159

[a] Set I, partial charges obtained by optimization of the electronic structure using GAUSSIAN;[43] set II, values for IRMOF-1 adapted to Cu-BTC;[42] sets III, IV, and V are set II increased by 2, 4, and 6%, respectively. The labeling of the atoms is shown in Figure 2.

Results and Discussion

We have considered several sets of partial charges for the atoms of Cu−BTC listed in Table 1. The initial atomic charges, labeled as set I, were taken from Frost and Snurr.[43] Set II was taken from available charges assigned to IRMOF-1,[42] where the charge of copper was adjusted to make the structure charge neutral. The other sets used in this work were obtained by increasing all of the charges of set II by 2, 4, and 6%, respectively.

Our first finding was that the computed water adsorption using set I was up to 600 times lower than the experimental values.[26] Our simulations show that, first, it is not possible to reproduce the experimental adsorption isotherm by increasing or decreasing the partial charges of only a few atom types (always keeping the total structure charge neutral), second, variations on the framework charges lead to a drastic change of the adsorption, and third, fixing the charge of Cu and changing the rest of the charges by a small amount did not influence the adsorption to a large extent. Therefore, to correctly reproduce the experimental adsorption of water in Cu−BTC, the charge of all atoms was changed simultaneously. As a starting point, we took the set of charges inherited from IRMOF-1 (set II) and generated new sets of charges, increasing all of the charges simultaneously in steps of 1% until the experimental isotherm was reproduced.

The isotherms obtained with different sets of atomic charges are compared with the experimental data at 295 K; see Figure 3. Set II qualitatively reproduces the linear trend of the experimental isotherm, but the adsorption is too low compared to that of the experiments of ref 26. The set labeled as IV exactly reproduces the experimental data. Compared to that of set II, the partial charge of the atoms of Cu−BTC is increased, making the interaction between the metal sites and water stronger and preserving the linear shape of the isotherm. Higher pressures were not included in Figure 3 due to the lack of accurate experimental data in that region. The saturation loading computed in our simulations equals 34 mol/kg. This result is

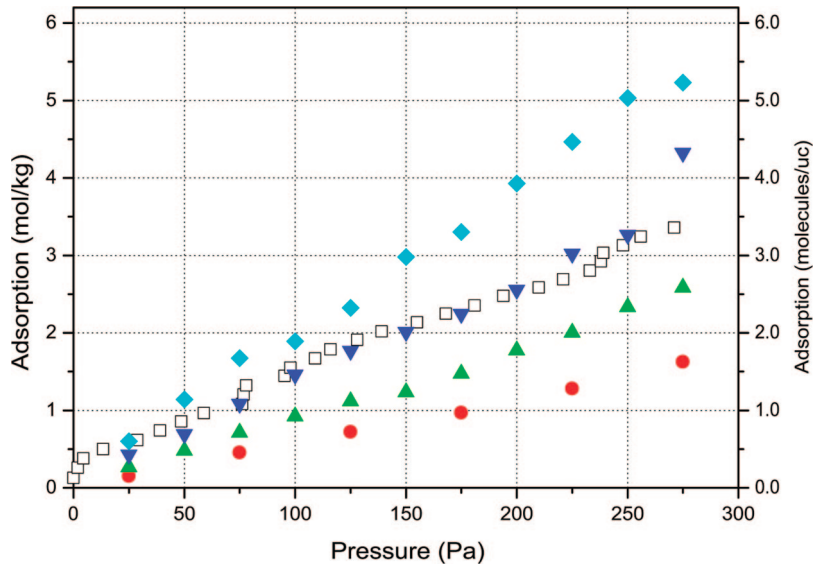

Figure 3. Adsorption isotherms of water in Cu−BTC at 295 K computed using the sets of partial charges of Table 1. Open squares, experimental data;[26] circles, charge set II; triangles up, charge set III; triangles down, charge set IV; diamond, charge set V. The isotherm for charge set I was not plotted because the adsorption was up to 600 times lower than the experimental values.

TABLE 2: The Various Contributions to the Interaction Energy of Water Adsorbed in Cu−BTC at Different Pressures and a Temperature of 295 K, Expressed in Parts Per Unit[a]

P (Pa)	*A*	*B*	*C*	*D*
25	0.01	0.99	0.81	0.81
50	0.02	0.98	0.85	0.85
75	0.02	0.98	0.84	0.84
100	0.03	0.97	0.88	0.83
125	0.05	0.95	0.84	0.84
150	0.05	0.95	0.87	0.87
175	0.06	0.94	0.84	0.84
200	0.08	0.92	0.86	0.85
225	0.11	0.89	0.87	0.86
250	0.13	0.87	0.88	0.87
275	0.19	0.81	0.89	0.87

[a] *A*: fraction of energy that corresponds to the water−water interaction; *B*: fraction of energy that corresponds to the water−Cu−BTC interaction; *C*: fraction of energy that is of electrostatic origin; *D*: fraction of electrostatic energy that corresponds to the water−Cu−BTC interaction.

quite large compared with available experimental data, 15,[44] 16,[22] and 22 mol/kg.[26] This difference can be explained by the fact that, in the simulations, the crystal structure is perfect while in the experiment it contains defects or trapped molecules that were not removed after the synthesis, and different methods and adsorption equipment were used.[45] In other simulation studies of MOFs, a scaling factor for the adsorption has been used to account for the pore volume really accessible to the experimental material.[46,47] This is supported by the fact that in our simulation, we measured a pore volume of 0.85 cm^3/g, measured using the Widom's test particle insertion method.[33] Experimental studies reported a pore volume of 0.69, 0.33, and 0.66 cm^3/g, respectively.[22,26,44]

In Table 2, we present the fraction of the total energy that corresponds to the water−water and to the water−MOF interactions for different pressures, as well as the fraction of the total and the water−MOF interaction that is of electrostatic origin. For all of the pressures considered, the total electrostatic energy is always larger than 80% of the total energy, and more than 80% of this is due to the water−MOF interactions. Furthermore, the total water−water interaction energy is always less than 20% of the total energy. This indicates that the adsorption is dominated by the electrostatic interaction between water and the framework atoms. This result may be surprising because water molecules interact via strong hydrogen bonds. The observation that the interactions between water molecules are weaker than those with the framework is corroborated with the computed enthalpies as a function of the loading. As shown in Figure 4, the heat of adsorption increases from 46 kJ/mol at zero coverage to 51 kJ/mol at around 4 molecules of water per unit cell, remaining almost constant from here to the loading of 42 molecules per unit cell. Note that this is significantly larger that the heat of vaporization of water.

Set IV has been additionally used to identify the preferential location of water in the structure. The main adsorption sites on this metal−organic framework were selected as explained by Liu et al.[48] for H_2 adsorption. Type-I sites were located near the copper atoms of the structure, type II sites were assigned to the center of the octahedral cages, and type III sites were located at the windows of the four open faces of the octahedral cage. In addition to these sites defined by Liu et al.,[48] we also considered the type-I′ adsorption site located in the big central cavities. To assign each adsorbed water molecule to an adsorption site, we have used a distance criterion with a cutoff radius of 0.2 nm for site II, a spherical annulus of radius 0.2 and 0.55 nm for site III (site II being at its center), and the one of site I as 0.3 nm, removing the intersection with site III, and finally, we defined site I′ as the rest of the volume not contained in the previous sites. In this way, every coordinate within the unit cell was assigned to one single site. The Cu−BTC structure with the defined adsorption sites is shown in Figure 1. According to our simulations, water adsorbs preferentially close to the Cu atoms at an average distance of 2.35 Å, which is close to the distance measured in ref 41 (2.19 Å). This is consistent with the fact that, after synthesis, Cu atoms are coordinated with water molecules[41] and that the metal sites of the MOF are activated when water is removed, allowing the adsorption of other molecules at those sites.[28] As we increase the pressure, the fraction of molecules close to the Cu atoms changes from 99% at 25 Pa to 82% at 275 Pa. The rest of the molecules increasingly adsorb by layers in the big cages of Cu−BTC on the preadsorbed water as the pressure rises, and a small amount

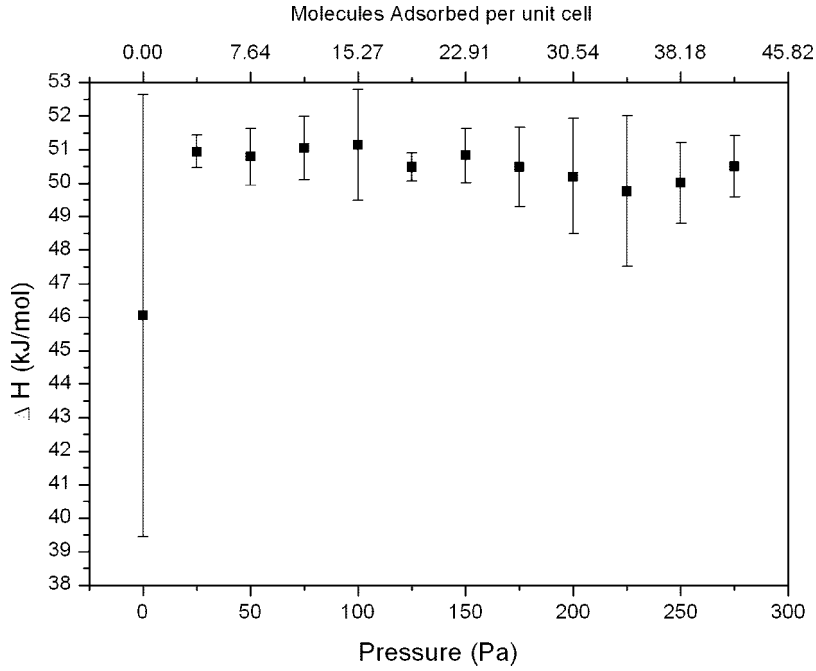

Figure 4. Absolute value of the heat of adsorption of water in Cu−BTC at 295 K as a function of loading.

TABLE 3: Calculated Henry Coefficients (mol kg^{-1} Pa^{-1}), Adsorption (Free) Energies (kJ mol^{-1}), Entropies (J mol^{-1} K^{-1}), and Enthalpies (kJ mol^{-1}) of the Adsorption of Water in Cu−BTC at 295 K for Different Adsorption Sites Using the Charge Set IV (See Table 1)[a]

site	K_H	ΔU	ΔH	ΔA	ΔG	ΔS
I	2.0×10^{-2} (5.3)	−45.6 (6.6)	−48.0 (6.6)	−26.6 (5.7)	−29.1 (5.7)	−65.6 (41.6)
I′	4.6×10^{-6} (0.2)	−14.0 (0.3)	−16.5 (0.3)	−5.6 (0.1)	−8.1 (0.1)	−28.4 (1.4)
III	5.7×10^{-6} (0.4)	−14.4 (0.4)	−16.8 (0.4)	−6.2 (0.2)	−8.6 (0.2)	−27.9 (1.9)
II + III	6.2×10^{-6} (0.2)	−14.2 (0.1)	−16.6 (0.1)	−6.4 (0.1)	−8.8 (0.1)	−26.5 (0.6)
total	1.3×10^{-2} (3.4)	−43.6 (3.9)	−46.1 (3.9)	−21.7 (3.1)	−24.2 (3.1)	−65.9 (23.6)

[a] The value in parentheses indicates the error in the last digits. For example, −45.6 (6.6) means −45.6 ± 6.6.

of them starts filling the channels of the octahedral cages. As every water molecule adsorbs close to one of the Cu atoms, it is expected that the heat of adsorption does not strongly depend on the loading. This is what we found for loadings up to 42 water molecules per unit cell. No molecules were observed in the neighborhood of the benzene groups or inside of the octahedral pockets. We obtained the same behavior using the charge set II. These results provide evidence that the metallic atoms of the Cu−BTC structure are a crucial factor for understanding the water adsorption.

The calculated Henry coefficients and the adsorption energies, entropies, and enthalpies are shown in Table 3 for the different adsorption sites of Cu−BTC. The Henry coefficient obtained for site I is four orders of magnitude larger than those for the other sites, while the energies, entropies, and enthalpies are three times lower in absolute value. These large differences between different sites are responsible for the large error bars obtained, especially for the values at zero loading. These values corroborate the strong preference of water for site I. It is interesting to highlight that the preferential adsorption site for water on Cu−BTC is completely different from those obtained for nonpolar and quadrupolar molecules. Water preferentially adsorbs on site I, whereas this site remains empty for hydrocarbons,[30,32] argon,[29] hydrogen,[30,48] nitrogen,[7] oxygen,[7] and carbon dioxide.[30] The preferential adsorption site for these molecules is at the interior of the octahedral cages (site II), while very few molecules adsorb in the neighborhood of the Cu atoms of the framework. Only hydrogen at low temperatures has shown a tendency to adsorb by the Cu atoms of the framework,[48] although the distance between the hydrogen and copper atoms has not been reported. To illustrate this point, Figure 5 shows the probability distribution of water, methane, and carbon dioxide adsorbed in Cu−BTC at low loading and 295 K. While water adsorbs mainly near the Cu atoms of the framework, methane and carbon dioxide adsorb preferentially at the interior of the octahedral cages, the big channels of Cu−BTC, and the windows of the side pockets, in that order.

Krungleviciute et al.[49] suggested that the preference of the molecules for adsorbing at the interior of the octahedral pockets is limited by the Lennard-Jones size parameter σ for interactions between the molecule and the carbon atoms of the MOF, so that Ar ($\sigma = 3.40$ Å) can adsorb at the interior of the octahedra while CF_4 ($\sigma = 3.99$ Å) cannot because of its value for σ. This explanation is not valid for the water model that we are using because, in our case, the maximum value of sigma for all the Lennard-Jones interactions in the system equals 3.28 Å, which is lower than the value for Ar, and therefore, it should be adsorbed at the interior of the octahedral cages. Our simulations show that the key to understand why the adsorption behavior of water in Cu−BTC is different that that to other molecules might be the dipole moment of the molecule. It has been previously suggested that Cu−BTC could be useful for separating molecules with different quadrupolar moments.[31] Molecular simulations have shown that in a carbon dioxide/nitrogen mixture, carbon dioxide tends to be closer to the Cu atoms of Cu−BTC due to its larger quadrupolar moment.[7] As water is

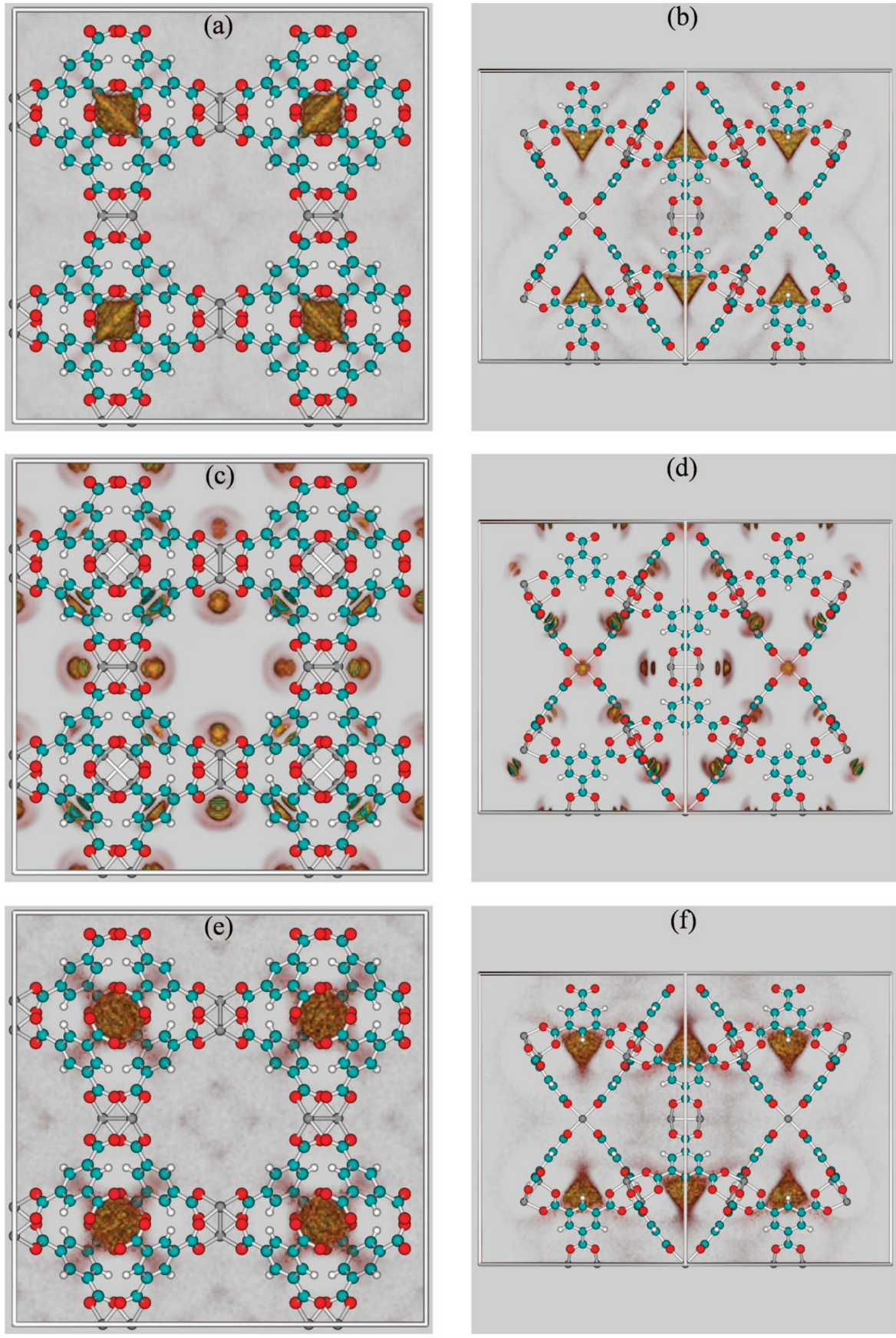

Figure 5. Snapshots showing the different adsorption preference of methane, water, and carbon dioxide in Cu−BTC at low loading. The data are taken from the pure component simulations of water at 25 Pa and methane and carbon dioxide at 2 kPa at 295 K. (a) Methane (front view); (b) methane (side view); (c) water (front view); (d) water (side view); (e) carbon dioxide (front view); (f) carbon dioxide (side view). While water adsorbs very close to the Cu atoms of Cu−BTC, the other two molecules adsorb at the center of the octahedral pockets, and the site close to the Cu atoms is completely empty, although some traces can be found at other locations. At these low loadings, we can find a weak coordination layer on the water molecules adsorbed on the Cu atoms and a complete absence of water at other adsorption sites. Additionally, water is much more concentrated at its main adsorption site than methane and carbon dioxide.

one of the molecules in nature with the largest dipolar moment, the affinity for the Cu atoms of the framework is expected to be larger, in agreement with our results. Furthermore, the extremely high sensitivity of the partial charge of Cu for water adsorption indicates that the metal sites of the MOFs are the essential element for understanding the adsorption of water in MOFs.

Acknowledgment. This work is supported by the Spanish "Ministerio de Educación y Ciencia (MEC)" (CTQ2007-63229), by the Junta de Andalucía (Excellence Project 2008-2010), and by The Netherlands Organization for Scientific Research (NWO-CW) through the VIDI grant of T.J.H.V. The authors wish to thank Houston Frost and Randall Q. Snurr for making the Cu−BTC framework charges available to us before publication and David Dubbeldam for fruitful discussions.

References and Notes

(1) Ferey, G. *Chem. Mater.* **2001**, *13*, 3084–3098.
(2) Batten, S. R. *Curr. Opin. Solid State Mater. Sci.* **2001**, *5*, 107–114.
(3) Rao, C. N. R.; Natarajan, R.; Vaidhyanathan, R. *Angew. Chem., Int. Ed.* **2004**, *43*, 1466–1496.
(4) Chae, H. K.; Siberio-Perez, D. Y.; Kim, J.; Go, Y.; Eddaoudi, M.; Matzger, A. J.; O'Keeffe, M.; Yaghi, O. M. *Nature* **2004**, *427*, 523–527.
(5) Rowsell, J. L. C.; Yaghi, O. M. *Angew. Chem., Int. Ed.* **2005**, *44*, 4670–4679.
(6) Pan, L.; Olson, D. H.; Ciemnolonski, L. R.; Heddy, R.; Li, J. *Angew. Chem., Int. Ed.* **2006**, *45*, 616–619.
(7) Yang, Q. Y.; Xue, C. Y.; Zhong, C. L.; Chen, J. F. *AIChE J.* **2007**, *53*, 2832–2840.
(8) Babarao, R.; Hu, Z. Q.; Jiang, J. W.; Chempath, S.; Sandler, S. I. *Langmuir* **2007**, *23*, 659–666.
(9) Batten, S. R.; Robson, R. *Angew. Chem., Int. Ed.* **1998**, *37*, 1460–1494.
(10) Eddaoudi, M.; Kim, J.; Rosi, N.; Vodak, D.; Wachter, J.; O'Keeffe, M.; Yaghi, O. M. *Science* **2002**, *295*, 469–472.
(11) Erxleben, A. *Coord. Chem. Rev.* **2003**, *246*, 203–228.
(12) Carlucci, L; Ciani, G.; Proserpio, D. M. *Coord. Chem. Rev.* **2003**, *246*, 247–289.
(13) Michaelides, A.; Skoulika, S.; Bakalbassis, E. G.; Mrozinski, J. *Cryst. Growth Des.* **2003**, *3*, 487–492.
(14) Gu, J. Z.; Lu, W. G.; Jiang, L.; Zhou, H. C.; Lu, T. B. *Inorg. Chem.* **2007**, *46*, 5835–5837.
(15) Zhao, H. K.; Ding, B.; Yang, E. C.; Wang, X. G.; Zhao, X. J. *Z. Anorg. Allgg. Chem.* **2007**, *633*, 1735–1738.
(16) Shi, Q.; Cao, R.; Sun, D. F.; Hong, M. C.; Liang, Y. C. *Polyhedron* **2001**, *20*, 3287–3293.
(17) Cao, R.; Sun, D. F.; Liang, Y. C.; Hong, M. C.; Tatsumi, K.; Shi, Q. *Inorg. Chem.* **2002**, *41*, 2087–2094.
(18) Fang, Q. R.; Zhu, G. S.; Xue, M.; Zhang, Q. L.; Sun, J. Y.; Guo, X. D.; Qiu, S. L.; Xu, S. T.; Wang, P.; Wang, D. J.; Wei, Y. *Chem.—Eur. J.* **2006**, *12*, 3754–3758.
(19) Greathouse, J. A.; Allendorf, M. D. *J. Am. Chem. Soc.* **2006**, *128*, 10678–10679.
(20) Li, Y.; Tang, R. *T Langmuir* **2007**, *23*, 12937–12944.
(21) Lin, X.; Blake, A. J.; Wilson, C.; Sun, X. Z.; Champness, N. R.; George, M. W.; Hubberstey, P.; Mokaya, R.; Schroder, M. *J. Am. Chem. Soc.* **2006**, *128*, 10745–10753.
(22) Chui, S. S. Y.; Lo, S. M. F.; Charmant, J. P. H.; Orpen, A. G.; Williams, I. D. *Science* **1999**, *283*, 1148–1150.
(23) Kitaura, R.; Kitagawa, S.; Kubota, Y.; Kobayashi, T. C.; Kindo, K.; Mita, Y.; Matsuo, A.; Kobayashi, M.; Chang, H. C.; Ozawa, T. C.; Suzuki, M.; Sakata, M.; Takata, M. *Science* **2002**, *298*, 2358–2361.
(24) Maji, T. K.; Ohba, M.; Kitagawa, S. *Inorg. Chem.* **2005**, *44*, 9225–9231.
(25) Kondo, A.; Daimaru, T.; Noguchi, H.; Ohba, T.; Kaneko, K.; Kanob, H. *J. Colloid Interface Sci.* **2007**, *314*, 422–426.
(26) Wang, Q. M.; Shen, D. M.; Bulow, M.; Lau, M. L.; Deng, S. G.; Fitch, F. R.; Lemcoff, N. O.; Semanscin, J. *Microporous Mater.* **2002**, *55*, 217–230.
(27) Zacher, D.; Baunemann, A.; Hermes, S.; Fischer, R. A. *J. Mater. Chem.* **2007**, *17*, 2785–2792.
(28) Panella, B.; Hirscher, M.; Putter, H.; Muller, U. *Adv. Funct. Mater.* **2006**, *16*, 520–524.
(29) Vishnyakov, A.; Ravikovitch, P. I.; Neimark, A. V.; Bulow, M.; Wang, Q. M. *Nano Lett.* **2003**, *3*, 713–718.
(30) Yang, Q. Y.; Zhong, C. L. *J. Phys. Chem. B* **2008**, *110*, 17776–17783.
(31) Liu, J. C.; Culp, J. T.; Natesakhawat, S.; Bockrath, B. C.; Sankar, S. G.; Garberoglio, G.; Johnson, J. K. *J. Phys. Chem. C* **2007**, *111*, 9305–9313.
(32) Wang, S. Y.; Yang, Q. Y.; Zhong, C. L. *Sep. Purif. Technol.* **2008**, *60*, 30–35.
(33) Frenkel, D.; Smit, B., *Understanding Molecular Simulation: From Algorithms to Applications*, 2nd ed.; Academic Press: San Diego, CA, 2002.
(34) Vlugt, T. J. H.; Krishna, R.; Smit, B. *J. Phys. Chem. B* **1999**, *103*, 1102–1118.
(35) Dubbeldam, D.; Calero, S.; Vlugt, T. J. H.; Krishna, R.; Maesen, T. L. M.; Smit, B. *J. Phys. Chem. B* **2004**, *108*, 12301–12313.
(36) Vlugt, T. J. H.; García-Pérez, E.; Dubbeldam, D.; Ban, S.; Calero, S. *J. Chem. Theory Comput.* **2008**, *4*, 1107–1118.
(37) Rick, S. *J. Chem. Phys.* **2004**, *120*, 6085–6093.
(38) Kell, G. S. *J. Chem. Eng. Data* **1975**, *20*, 97–105.
(39) Mayo, S. L.; Olafson, B. D.; Goddard, W. A. *J. Phys. Chem.* **1990**, *94*, 8897–8909.
(40) Rappe, A. K.; Casewit, C. J.; Colwell, K. S.; Goddard, W. A.; Skiff, W. M. *J. Am. Chem. Soc.* **1992**, *114*, 10024–10035.
(41) Prestipino, C.; Regli, L.; Vitillo, J. G.; Bonino, F.; Damin, A.; Lamberti, C.; Zecchina, A.; Solari, P. L.; Kongshaug, K. O.; Bordiga, S. *Chem. Mater.* **2006**, *18*, 1337–1346.
(42) Dubbeldam, D.; Walton, K. S.; Ellis, D. E.; Snurr, R. Q. *Angew. Chem., Int. Ed.* **2007**, *46*, 4496–4499.
(43) Frost, H.; Snurr, R. Q. Personal communication.
(44) Li, Y.; Tang, R. T. *AIChE J.* **2008**, *54*, 269–279.
(45) Mueller, U.; Schubert, M.; Teich, F.; Puetter, H.; Schierte-Arndt, K.; Paste, J. *J. Mater. Chem.* **2006**, *16*, 626–636.
(46) Surble, S.; Millange, F.; Serre, C.; Duren, T.; Latroche, M.; Bourrelly, S.; Llewellyn, P. L.; Ferey, G. *J. Am. Chem. Soc.* **2006**, *128*, 14889–14896.
(47) Dubbeldam, D.; Frost, H.; Walton, K. S.; Snurr, R. Q. *Fluid Phase Equilib.* **2007**, *261*, 152–161.
(48) Liu, Y.; Brown, C. M.; Neumann, D. A.; Peterson, V. K.; Kepert, C. J. *J. Alloys Compd.* **2007**, *446*, 385–388.
(49) Krungleviciute, V.; Lask, K.; Migone, A. D.; Lee, J.-Y.; Li, J. *AIChE J.* **2008**, *54*, 918–923.

JP806363W